

# Assembly Sequences Based on Multiple Criteria Against Products with Deformable Parts

Takuya Kiyokawa, Jun Takamatsu, and Tsukasa Ogasawara

**Abstract**—This study investigates assembly sequence generation by considering two tradeoff objectives: (1) insertion conditions and (2) degrees of constraints among assembled parts. A multiobjective genetic algorithm is used to balance these two objectives for planning robotic assembly. Furthermore, the method of extracting part relation matrices including interference-free, insertion, and degree of constraint matrices is extended for application to 3D computer-aided design (CAD) models, including deformable parts. The interference of deformable parts with other parts can be easily investigated by scaling models. A simulation experiment was conducted using the proposed method, and the results show the possibility of obtaining Pareto-optimal solutions of assembly sequences for a 3D CAD model with 33 parts including a deformable part. This approach can potentially be extended to handle various types of deformable parts and to explore graspable sequences during assembly operations.

**Index Terms**—Robotic Assembly, Assembly Sequence, CAD, Constraint, Deformable Object

## I. INTRODUCTION

PRODUCTION systems that can respond quickly and flexibly to changes in market demands are needed urgently [1]. To achieve an automated-product manufacturing line, assembly sequences must be generated rapidly. Studies have focused on using 3D computer-aided design (CAD) models at the product design stage for automatic assembly sequence generation [2], [3].

The combinatorial optimization problem of determining the assembly sequence of parts in a product is known to be an NP-hard problem [4]. Heuristic search methods have been used to obtain a quasi-optimal solution to find a feasible assembly sequence in a realistic time. Some researchers have applied methods using a genetic algorithm (GA) [5] and extended algorithms [6], [7] to plan the assembly of parts in two dimensions and generated a feasible assembly sequence in such a limited situation. Pan *et al.* [8] generated multiple assembly sequences from a STEP file, a type of 3D CAD file; however, the final assembly sequence had to be determined manually.

Tariki *et al.* [9] generated assembly sequences with a large number of parts (e.g., 32) by improving the initial chromosomes of the GA. Tariki *et al.* [10] extended the previous method to handle the insertion (e.g., male-female) relationship.

However, in the assembly sequence generated by considering only the interference and insertion conditions between parts, there exists a sequence in which the insertion of a certain

All authors are with Division of Information Science, Robotics Laboratory, Nara Institute of Science and Technology (NAIST), Japan {kiyokawa.takuya.kj5, j-taka, ogasawar}@is.naist.jp

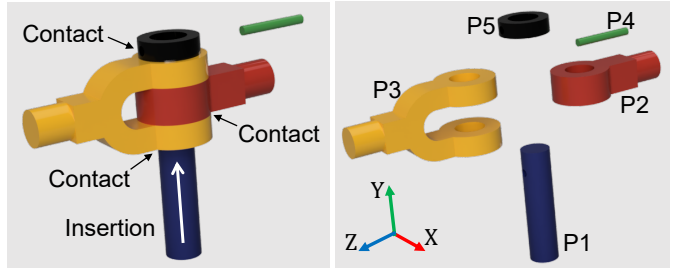


Fig. 1: Inserting a part that causes many constraints

part is simultaneously constrained by several parts, as shown in the left-hand side of Fig. 1. Such insertions are considered difficult to handle. The assembly sequence generation for models with deformable objects is another issue that must be solved. All aforementioned methods can only handle rigid parts.

The planning of assembly operations such that they proceed smoothly considering the target object constrained by contacts between the object and the surrounding object is considered a basic problem [11]–[14]. This problem has been focused on in the planning of robotic assembly based on contact state transitions defined by the infinitesimal displacement of objects [15], [16].

Hirai *et al.* [17] proposed a network representation of contact states between parts in the assembly process and analyzed the kinematics of the object to be manipulated by considering the mechanical contact represented by inequalities using the theory of convex polyhedral cones. Yoshikawa *et al.* [18] defined the constraints of the contact state based on infinitesimal feasible translational and rotational displacements. They chose an assembly sequence from several possible transitions of the contact states where the degree of constraints is increased slightly.

The task of inserting a part, as shown in Fig. 1, is difficult because of the difficulty in constraint state transitions. In this study, we designed the fitness function of an assembly sequence based on constraint state transitions to reduce such difficulties in transitions.

For determining the assembly sequence, we designed a function to evaluate the assembly sequences that satisfy the conditions of insertion and constraint state transition to consider the planning of assembly operations. As there is a tradeoff relationship between the two conditions, we solved *multiobjective optimization problems* (MOPs) based on two objective functions. Thus far, multicriteria assembly sequencing has been tried using given datasets of a product including

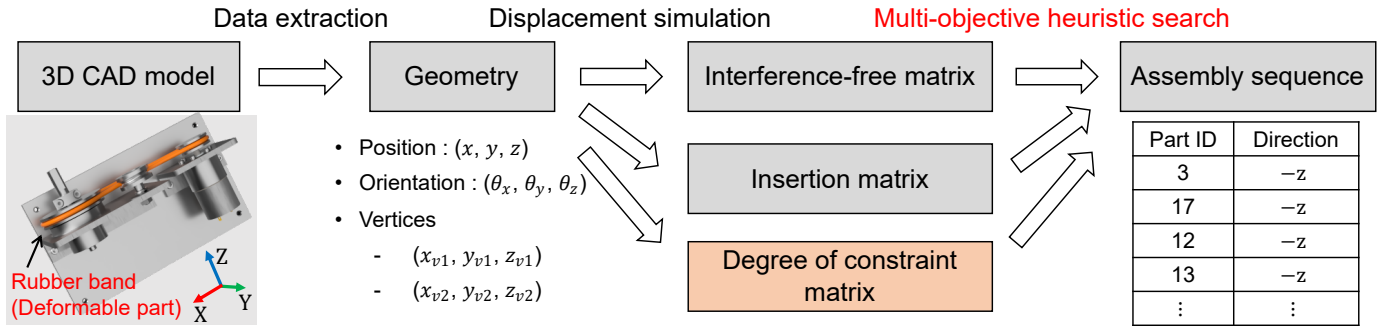


Fig. 2: Overview of generating an assembly sequence from a 3D CAD model

19 parts [19]. This study focused on minimizing production time and cost. Previous studies did not discuss criteria to reduce the difficulty of assembly operations and how to extract necessary information from models and handle deformable parts.

We performed multiobjective optimization using a *multiobjective GA* (MOGA) [20] under the designed fitness function to investigate the possibility of finding a Pareto-optimal solution for an assembly sequence. This study also proposes an automatic method for extracting the interference-free, insertion, and degree of constraint matrices for a product including deformable parts by using a 3D model. In our experiments, we demonstrate the effectiveness of the proposed method by applying it to an assembly consisting of 33 parts including a deformable rubber band.

## II. ASSEMBLY SEQUENCE GENERATION

### A. Exploring Quasi-optimal Sequence using a 3D CAD Model

Fig. 2 summarizes the procedure of generating an assembly sequence from the assembled models. First, the system extracts the geometric information of the assembly parts from the CAD model, and then the proposed algorithm calculates the interference-free, insertion, and proposed degree of constraint matrices. Next, the assembly sequences are generated to satisfy the conditions of the insertion relation and constraint state transition. In practice, based on the proposed fitness function, we used our proposed system to conduct multiobjective optimization of the assembly sequence using the proposed MOGA.

### B. Extraction of Part Relations between Rigid Parts

We extract geometric information from CAD models using the CAD software and calculate the interference-free and insertion matrices of rigid body parts based on the method proposed by Tariki *et al.* [9], [10]. In this section, we describe a method for extracting the interference-free information and constructing the proposed degree of constraint matrix for calculating the contact state transition difficulty of rigid parts.

The interference-free information of an arbitrary part is determined by investigating whether a part interferes with other parts, as illustrated in Fig. 3. In the figure, the investigated target part is displaced in six positive and negative directions along the X Y and Z axes and rotated around the X, Y and Z axes as rotation axes.

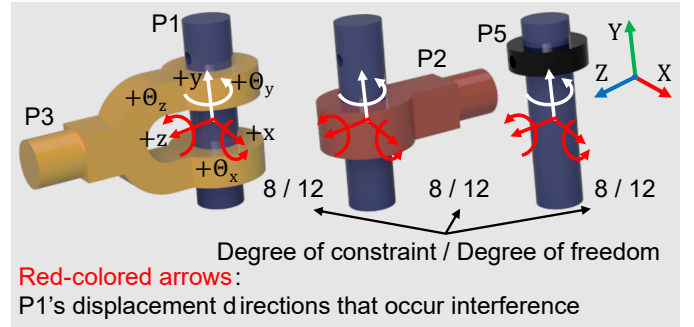


Fig. 3: Degree of constraint of parts

This paper describes a method for calculating degree of constraint  $C(P_i, P_k)$  that indicates the contact state between parts  $P_i$  and  $P_k$  during their assembly. If there is no contact between these parts, this value is set to 0. According to the degree of constraint defined by Yoshikawa *et al.* [18], if  $P_1, P_2, \dots, P_\eta$  (where  $\eta$  is the number of parts) indicate parts identified by IDs, the following equation is applicable:

$$C(P_i, P_k) = 12 - \sum_{j=1}^{12} F_j(P_i, P_k) \in \{0, 1, \dots, 12\} \quad (1)$$

where  $F_j$  ( $j = 1, 2, \dots, 12$ ) indicates interference-free information. In this case, the interference-free information is for 12 directions of translational displacements  $\pm x, \pm y, \pm z$  and rotational displacements  $\pm \theta_x, \pm \theta_y, \pm \theta_z$ , as shown in Fig. 3. This value is set as 1 if the parts do not interfere with each other after a displacement and as 0 if they do. Finally, the degree of constraint matrix is then computed using Equation (1) as an element.

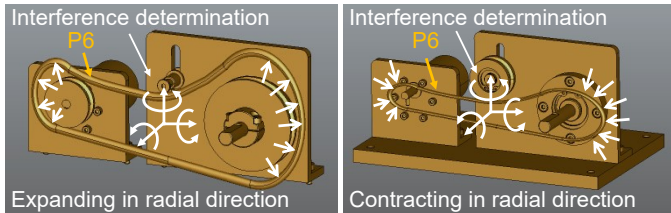
### C. Extraction of Part Relations for a Deformable Part

By considering a rubber band as an example, we describe the extraction of interference-free information for deformable objects with the 12 directions. We assumed that the deformability of a part could easily be determined based on the part name.

For example, P6 shown in Fig. 4 is a rubber band that transmits the rotation of the motor shaft to another pulley and is a deformable object. In general, a rubber band must be stretched and retracted in the radial direction when attached to a pulley groove in the assembly as humans do (Fig. 4 (a)).



(a) Avoiding interference by deforming the object



(b) Determination of interference

Fig. 4: Determination of interference for a deformable object

TABLE I: GA parameters used in our experiments

Parameter	Value
Number of chromosomes	$\eta$
Crossover rate	0.2
Mutation rate	0.1
Cut-and-paste rate	0.35
Break-and-join rate	0.35
Number of generations	100
Number of iterations of GA	10

If the deformable object expands and contracts in the radial direction, the interference-free information of its deformable shape is extracted in the radial direction, as shown in Fig. 4 (b). The case in which all interference-free information is zero was not considered because such a scenario indicates that assembly is infeasible in any sequence. We changed the scaling parameters for the deformations, and if one of the extracted interference-free information with 12 directions becomes 1, the scaling parameters were adopted. By this scaling method, the interference-free information for 12 directions for the deformable object is extracted, and then, the interference-free and degree of constraint matrices that were obtained as in the case of the rigid body are generated. In addition, an insertion matrix was also generated from the deformable model by using the same method as that used for the rigid body.

#### D. Optimization using MOGA

For multiobjective optimization of assembly sequences, we built an algorithm based on NSGA-II [21], an MOGA that provides high search performance for 2–3 objective MOPs. The proposed algorithm is illustrated in Fig. 5. In this study, the method used by Tariki *et al.* [10], which has been suggested to be effective in optimizing the assembly sequence, was used for chromosome coding, chromosome initialization, and genetic operation.

The fitness function is designed such that if the assembly is infeasible, the evaluation is the lowest; otherwise, it is designed such that the sequence with the lowest difficulty level

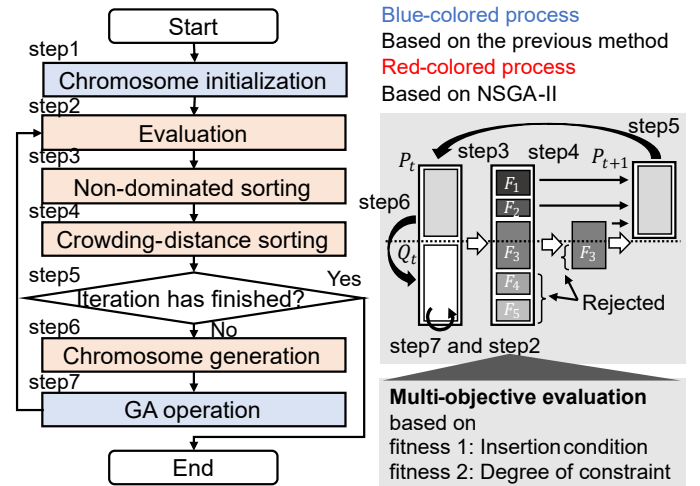


Fig. 5: Algorithm of assembly sequence optimization

of constraint state transition receives the highest evaluation during the assembly of each part. Minimizing the difficulty of the constraint state transition must be solved for each part assembly. Specifically,

$$f_c := \begin{cases} 12(\eta - 1) - H & \text{feasible} \\ 0 & \text{infeasible} \end{cases} \quad (2)$$

denotes a fitness function for the difficulty of the constraint state transition. This value is fixed as 0 for infeasible assembly. The feasibility of a sequence is determined using the method of Smith *et al.* [5]. In Equation (2),  $\eta$  is the number of parts and  $H$  is the maximum value of the constraint state transition difficulty for the assembly of each part. Then,  $H$  is calculated using the degree of constraint  $C$  of Equation (1) as follows:

$$H := \max_{k \in \{2, 3, \dots, \eta\}} \sum_{i=1}^{k-1} C(P_{O_i}, P_{O_k}), \quad (3)$$

where  $\sum_{i=1}^{k-1} C(P_{O_i}, P_{O_k})$  shows the constraint state transition difficulty in the assembly of the  $k$ -th part  $P_{O_k}$  and the other assembled parts  $P_{O_1}, P_{O_2}, \dots, P_{O_{k-1}}$ . According to the definition, the maximum constraint of two parts is 12; therefore,  $H$  in Equation (2) is less than  $12(\eta - 1)$ .

The fitness function for generating the assembly sequence that satisfies the insertion condition uses the following equation proposed by Tariki *et al.* [10].

$$f_i(s) := \begin{cases} 2\eta + \alpha(s) - \beta(s) - r(s) & \text{feasible} \\ \eta/2 & \text{infeasible} \end{cases}, \quad (4)$$

where  $s$  indicates the assembly sequence,  $\alpha(s)$  and  $\beta(s)$  are parameters related to the insertion condition, and  $r(s)$  is the number of changes in the assembly direction. Using the same method in case of Equation (2), if the assembly sequence is infeasible, the extracted interference-free information is used to determine the possibility of an assembly.

### III. EXPERIMENTS

#### A. Outline

Two case studies were conducted using two types of CAD files. Case Study 1 used a CAD file including the assembled

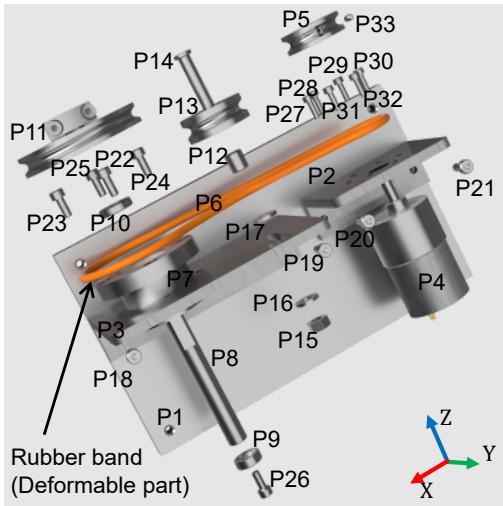


Fig. 6: Belt drive unit used in Case Study 2

model of the parts shown in the right-hand side of Fig. 1 to check whether the problem shown in the left-hand side of Fig. 1 can be resolved. Case Study 2 used a CAD file of the belt drive unit (Fig. 6) comprising 33 parts used in the World Robot Summit 2018 [22]. Using this model, we investigated the possibility of automatically generating the assembly sequence for a product with a large number of parts, including the rubber band shown in Fig. 6. The GA was applied with the parameters shown in Table I.

### B. Case Study 1

Fig. 7 shows the assembly sequence with the highest sum of the fitness values of Equation (2) and Equation (4) among the assembly sequences of 10 trials. The sequence shown in the left-hand side in Fig. 1, depicting the simultaneous occurrence of contacts, is not generated; however, the assembly sequence with a low constraint state transition difficulty was generated in the assembly of each part. Fig. 1 (left) shows that when P1 is inserted, constraints occur simultaneously on P2, P3, and P5, and the constraint state transition difficulty is 24 ( $= 8 + 8 + 8$ ).

In contrast, when P1 is inserted, as shown in Fig. 7, constraints occur between P3 and P5, and the constraint state transition difficulty is 16 ( $= 8 + 8$ ). In the insertion of P5, the constraints with only P1 and P3 are 13 ( $= 8 + 5$ ). In both these cases, the difficulty level of constraint state transition is less than 24. The assembly of the other parts also shows a difficulty level of less than 16; thus, the maximum value of the constraint state transition difficulty could be reduced from 24 to 16.

### C. Case Study 2

Fig. 8(a) shows the fitness values of Equation (4) and Equation (2) (fitness 1 and 2, respectively) of the 33 generated assembly sequences ( $= \eta$ ). Both these fitness values are over  $16.5 = \eta/2$  in all generated sequences, and an interference-free sequence was generated in the assembly of all parts

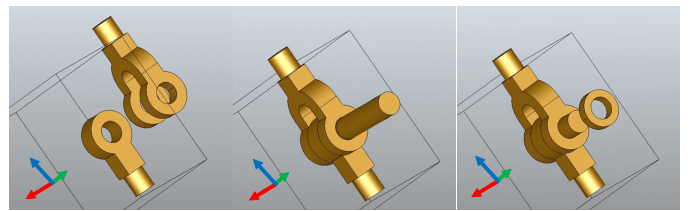


Fig. 7: Generated sequence in Case Study 1

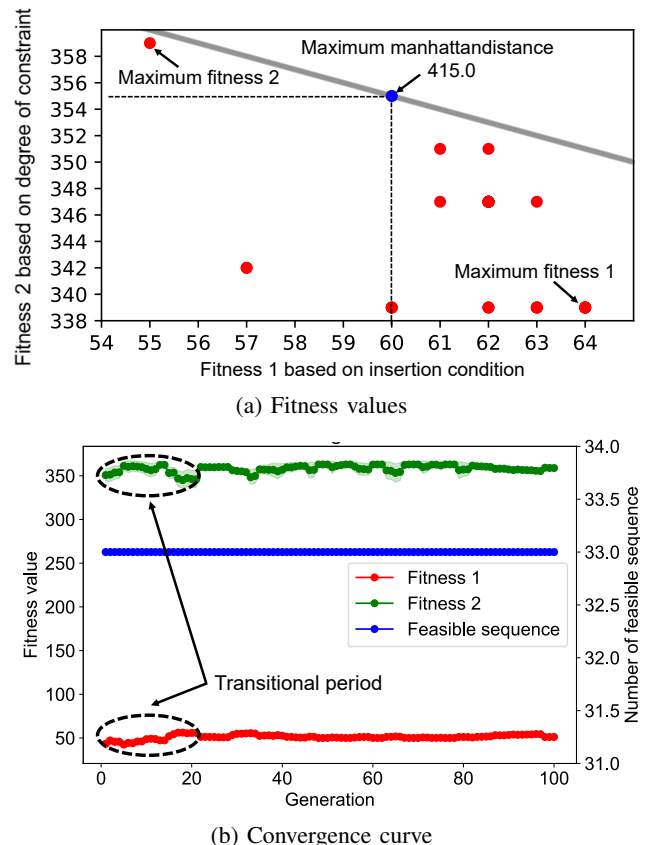


Fig. 8: Simulation results of Case Study 2

including the deformable object. If these depict weak Pareto-optimal solutions, the solution near the blue point in Fig. 8(a), where the sum of both fitness values is the maximum, is likely to be a Pareto-optimal solution. These results suggest that it is possible to search for a Pareto-optimal solution by using the proposed method.

Fig. 8(b) shows the convergence curve of the GA. The graph shows three curves of the mean with standard deviation of the fitness values with respect to fitness 1 (red curve) and fitness 2 (green curve) as well as the number of feasible sequences. The number of feasible sequences was constant at 33, indicating that 100% of the generated sequences are feasible. It is possible that the values may have converged to quasi-optimal values during the first generation update. An unsteady variation is observed in the evaluated values until near the 20th generation update after which the fitness values of the generated sequences are stable and produce high fitness values.

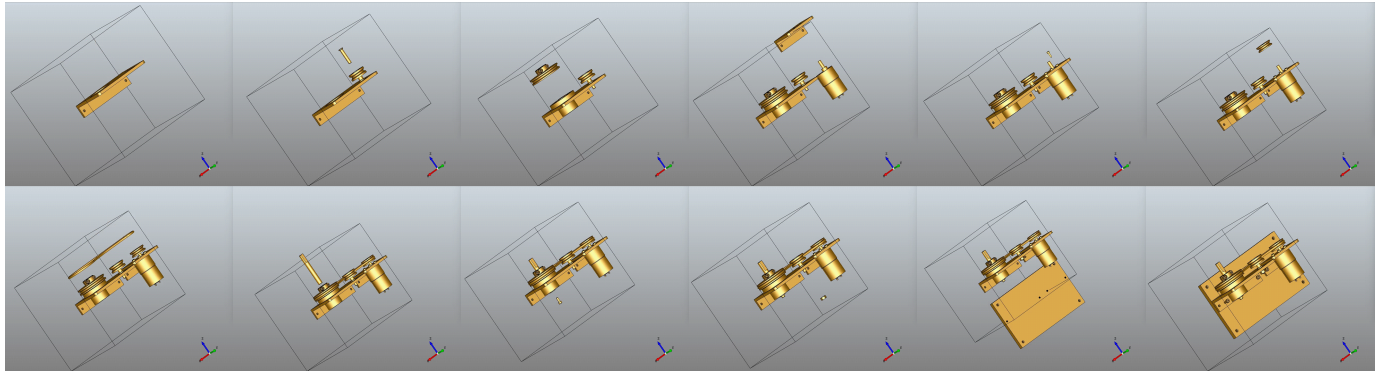


Fig. 9: Generated sequence in Case Study 2

Fig. 9 shows the generated sequence with the highest fitness value depicted in the blue circle in Fig. 8(a). P5 in the generated sequence shows the maximum sum of both fitness values. Considering only insertion conditions, it is better to assemble P5 and P2 before P4. However, the insertion of P4 into P5 and P2 is constrained. In the proposed method, P5 is assembled last, and the difficulty of constraint state transition in the assembly of P2, P4, and P5 was reduced.

#### IV. DISCUSSION

##### A. Versatility to Variation of Deformable Shapes

Fig. 10 shows the other deformable objects used in the assembly challenge of WRS2018 [23] or that will be used in the assembly challenge of WRS2020 [24].

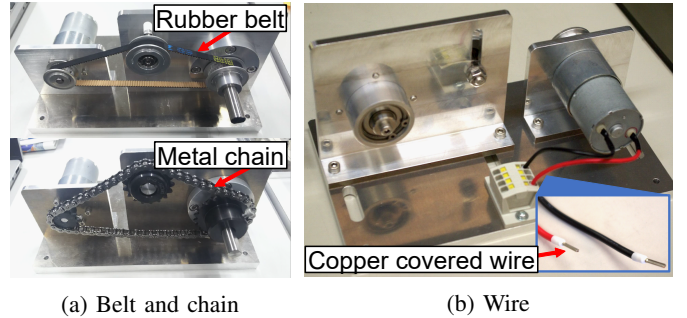
An extraction method is required for linear deformable objects, such as the wire used in this verification (Fig. 10(b)), instead of the proposed method that is used for circular deformable objects such as the rubber band (Fig. 6), rubber belt, and metal chain (Fig. 10(a)).

As shown in Fig. 11, unless it is just a string, many linear deformable parts, such as a cable with a plug or a wire with pins (Fig. 11), can be inserted into or connected to other parts, with a rigid body often attached to the tip. Therefore, if the linear deformable object has a rigid part connected to other objects, the interference for the rigid part with the other objects must be investigated. Linear deformable objects, such as connectors, cables and wires, also appear frequently in assemblies.

For example, the vertices of the linear objects and the corresponding female part are recognized, and then, the system determines the interference between them. This implies that the deformable part in linear deformable objects is disregarded. The entanglement with other parts after the approach needs to be considered; however, this is beyond the scope of the present study.

##### B. Graspable Sequences

Once the assembly sequence is determined, the grasping and assembly operation by a robot arm must be planned; for this, the feasible grasping point must be determined based on the specifications of the robot arm.



(a) Belt and chain

(b) Wire

Fig. 10: Deformable parts used in [23] (a) and to be used in [24] (b)

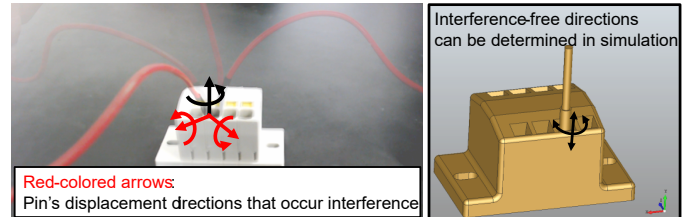


Fig. 11: Determination of interference for a wire in a hole

Fig. 12 illustrates an easy approach for determining the grasping point. Fig. 12 (a) and (b) demonstrate the graspability with a sequence generated in Case Study 1. We used a parallel two-finger gripper (ROBOTIQ, Hand-E) that was developed for precise assembly operations. The following procedure was performed.

- 1) Random sampling of hand-crafted graspable space on the object surface
- 2) Generating concatenated models of the parts and the gripper by using a certain pose of the gripper
- 3) Determining the interference by moving the concatenated models in the simulation using CAD models

By using a CAD model-based simulation to evaluate the interference, similar to the method of assembly sequence generation, it is possible to determine whether interference exists in the sequence of all parts. The random sampling of the graspable space can be replaced with the current vision-based grasp point detection method [25].

As the output of the GA can produce multiple sequences

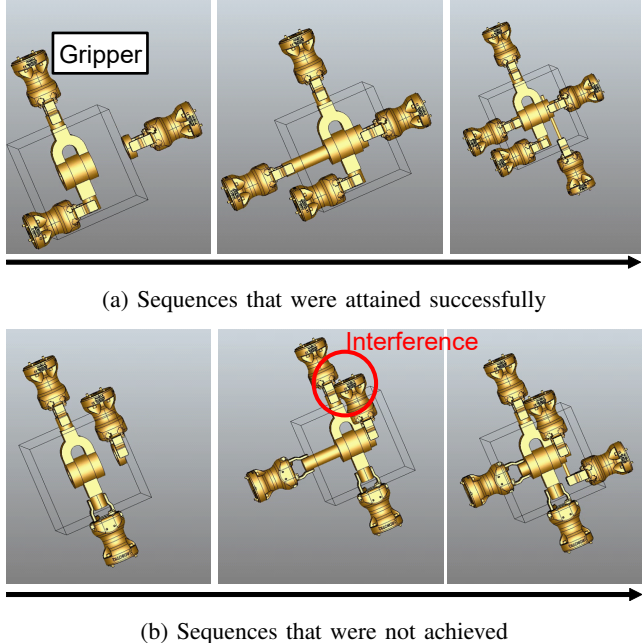


Fig. 12: Simulation results for graspable sequences

with the same high fitness value, the method can be extended to examine whether such a value could be achieved, for example, by using a CAD model of a robot gripper and hand, for multiple sequences.

## V. CONCLUSION

In this study, we designed a fitness function based on the level of constraint state transition difficulty to generate assembly sequences from a CAD model by considering the planning of assembly operations. We proposed the use of a multiobjective genetic algorithm along with the previously proposed insertion condition to solve this problem. In addition, we propose a method for extracting interference-free information based on the displacement of a deformable object by deforming the 3D model as well as a rigid body. By using the proposed method, we could compute the interference-free, insertion, and degree of constraint matrices for deformable objects.

In an experiment of assembly sequence generation, the results were applied to an assembly consisting of 33 parts including a deformable object, suggesting the possibility of searching for a Pareto-optimal solution of the assembly sequence, considering the planning of assembly operations.

In the future, we will clarify the possibility of determining the assembly sequence from the Pareto-optimal solution based on the planning of robotic assembly by considering the grasping potential of the parts as proposed by Wan *et al.* [26].

## REFERENCES

- [1] A. Gunasekaran, Y. Y. Yusuf, E. O. Adeleye, T. Papadopoulos, D. Kovvuri, and D. G. Geyi, “Agile manufacturing: an evolutionary review of practices,” *Int. J. of Production Research*, vol. 57, no. 15-16, pp. 5154–5174, 2019.
- [2] M. V. A. R. Bahubalendruni and B. B. Biswal, “A review on assembly sequence generation and its automation,” *J. of Mechanical Engineering Science*, vol. 230, no. 5, pp. 824–838, 2015.
- [3] B. B. V. L. Deepak, G. B. Murali, M. V. A. R. Bahubalendruni, and B. B. Biswal, “Assembly sequence planning using soft computing methods: A review,” *Proc. of Institution of Mechanical Engineers, Part E: J. of Process Mechanical Engineering*, vol. 233, no. 3, pp. 653–683, 2019.
- [4] M. Golwasser, J.-C. Latombe, and R. Motwani, “Complexity measures for assembly sequences,” *Int. J. of Computational Geometry & Applications*, vol. 9, no. 4-5, pp. 371–417, 1999.
- [5] S. S.-F. Smith, G. C. Smith, and X. Liao, “Automatic stable assembly sequence generation and evaluation,” *J. of Manufacturing Systems*, vol. 20, no. 4, pp. 225–235, 2001.
- [6] S.-F. Chen and Y.-J. Liu, “An adaptive genetic assembly-sequence planner,” *Int. J. of Computer Integrated Manufacturing*, vol. 14, no. 5, pp. 489–500, 2001.
- [7] G. C. Smith and S. S.-F. Smith, “An enhanced genetic algorithm for automated assembly planning,” *Robotics and Computer Integrated Manufacturing*, vol. 18, no. 5-6, pp. 355–364, 2002.
- [8] C. Pan, S. S.-F. Smith, and G. C. Smith, “Automatic assembly sequence planning from STEP CAD files,” *Int. J. of Computer Integrated Manufacturing*, vol. 19, no. 8, pp. 775–783, 2006.
- [9] K. Tariki, T. Kiyokawa, T. Nagatani, J. Takamatsu, and T. Ogasawara, “3D model-based non-interference assembly sequence generation for products with a large number of parts,” in *CIS-RAM*, 2019, pp. 167–172.
- [10] K. Tariki, T. Kiyokawa, G. A. G. Ricardez, J. Takamatsu, and T. Ogasawara, “3D model-based assembly sequence optimization using insertion properties of parts,” in *SII*, 2020, pp. 1400–1405.
- [11] H. Hirukawa, T. Matsui, and K. Takase, “A general algorithm for derivation and analysis of constraint for motion of polyhedra in contact,” in *Workshop on IROS*, 1991, pp. 38–43.
- [12] H. Hirukawa and K. Iwata, “Recognition of contact state based on geometric model,” in *ICRA*, 1991, pp. 1507–1512.
- [13] Y. Yokokohji, Y. Yu, N. Nakasu, and T. Yoshikawa, “Quasi-dynamic manipulation of constrained object by robot fingers in assembly tasks,” in *IROS*, 1993, pp. 144–151.
- [14] Y. Yu, Y. Yokokohji, and T. Yoshikawa, “Two kinds of degree of freedom in constraint state and their application to assembly planning,” in *ICRA*, 1996, pp. 1993–1999.
- [15] K. Ikeuchi and T. Suehiro, “Toward an assembly plan from observation Part I: Task recognition with polyhedral objects,” *IEEE Trans. on Robotics and Automation*, vol. 10, no. 3, pp. 368–385, 1994.
- [16] J. Takamatsu, K. Ogasawara, H. Kimura, and K. Ikeuchi, “Recognizing assembly tasks through human demonstration,” *The Int. J. of Robotics Research*, vol. 26, no. 7, pp. 641–659, 2007.
- [17] S. Hirai, “Analysis and planning of manipulation using the theory of polyhedral convex cones,” Ph.D. dissertation, Kyoto University, 1991.
- [18] T. Yoshikawa, Y. Yokokohji, and Y. Yu, “Assembly planning operation strategies based on the degree of constraint,” in *IROS*, 1991, pp. 682–687.
- [19] Y.-K. Choi, D. M. Lee, and Y. B. Cho, “An approach to multi-criteria assembly sequence planning using genetic algorithms,” *The Int. J. of Advanced Manufacturing Technology*, vol. 42, pp. 180–188, 2009.
- [20] C. A. C. Coello, D. A. V. Veldhuizen, and G. B. Lamont, *Evolutionary Algorithms for Solving Multi-Objective Problems*. New York: Kluwer Academic Publishers, 2002.
- [21] K. Deb, A. Pratap, S. Agarwal, and T. Meyarivan, “A fast elitist multiobjective genetic algorithm: NSGA-II,” *IEEE Trans. on Evolutionary Computation*, vol. 6, no. 2, pp. 182–197, 2002.
- [22] Y. Yokokohji, Y. Kawai, M. Shibata, Y. Aiyama, S. Kotosaka, W. Uemura, A. Noda, H. Dobashi, T. Sakaguchi, and K. Yokoi, “Assembly challenge: a robot competition of the industrial robotics category, world robot summit – summary of the pre-competition in 2018,” *Adv Robot*, vol. 33, no. 17, pp. 876–899, 2019.
- [23] “Industrial robotics category assembly challenge rules and regulations 2018,” The Industrial Robotics Competition Committee, October 2018. [Online]. Available: [https://worldrobotsummit.org/download/rulebook-en/rulebook-Assembly\\_Challenge.pdf](https://worldrobotsummit.org/download/rulebook-en/rulebook-Assembly_Challenge.pdf)
- [24] “Industrial robotics category assembly challenge rules and regulations 2020,” The Industrial Robotics Competition Committee, January 2020. [Online]. Available: [https://worldrobotsummit.org/wrs2020/challenge/download/Rules/DetailedRules\\_Assembly\\_EN.pdf](https://worldrobotsummit.org/wrs2020/challenge/download/Rules/DetailedRules_Assembly_EN.pdf)
- [25] J. Mahler, J. Liang, S. Niyaz, M. Laskey, R. Doan, X. Liu, J. A. Ojea, and K. Goldberg, “Dex-net 2.0: Deep learning to plan robust grasps with synthetic point clouds and analytic grasp metrics,” in *RSS*, 2017.
- [26] W. Wan, K. Harada, and K. Nagata, “Assembly sequence planning for motion planning,” *Assembly Automation*, vol. 38, no. 2, pp. 195–206, 2018.